JCTC Journal of Chemical Theory and Computation

Article

pubs.acs.org/JCTC

First-Principles Study on Structural and Chemical Asymmetry of a Biomimetic Water-Splitting Dimanganese Complex

Ting Zhou,[†] Xiangsong Lin,[‡] and Xiao Zheng*,[†,§]

[†]Hefei National Laboratory for Physical Sciences at the Microscale, University of Science and Technology of China, Hefei, Anhui 230026, China

[‡]State Key Laboratory of Molecular Reaction Dynamics and Center for Theoretical Computational Chemistry, Dalian Institute of Chemical Physics, Chinese Academy of Sciences, Dalian, Liaoning 116023, China

[§]Guizhou Provincial Key Laboratory of Computational Nano-Material Science, Institute of Applied Physics, Guizhou Normal College, Guiyang, Guizhou 550018, China

Supporting Information

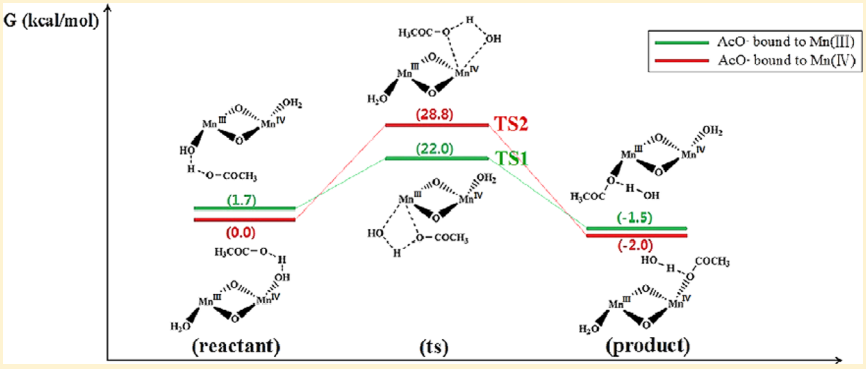

ABSTRACT: Density-functional theory calculations are carried out for a biomimetic dimanganese complex, $[H_2O(terpy)Mn^{III}(\mu\text{-}O)_2Mn^{IV}(terpy)OH_2]^{3+}$(**1**, terpy = 2,2′:6′,2″-terpyridine), which is a structural model for the oxygen evolving center of photosystem II. Theoretical investigations aim at elucidating the asymmetry features in the geometric and electronic structures of complex **1**, as well as their influences on the chemical functions of the two manganese centers, in the presence of water solvent. With the insight gained from the first-principles calculations, we study the oxidation state of complex **1** in the acetate buffer solution. Both the thermodynamic and kinetic aspects are explored in detail, and the structural and chemical asymmetry of the two manganese centers is fully considered. It is found that the larger steric repulsion associated with the Mn(IV) center plays a decisive role, which leads to the predominant acetate coordination at the Mn(III) ion. This thus resolves the existing controversy on the preferential acetate binding to complex **1**.

I. INTRODUCTION

Synthesizing biomimetic systems which realize the chemical functionality and efficiency of photosystem II (PS II), the solar water-splitting protein complex, is a highly desirable goal for scientists.[1−4] A vast amount of efforts, both in experiments and in theory, have been devoted to achieving this goal. In particular, much work has been done to understand the structure and properties of the oxygen evolving center (OEC) of PS II, which contains a tetranuclear manganese−calcium-oxo (Mn_4Ca-oxo) catalytic cluster.[5−9] The structure and oxidation state of the Mn_4Ca cluster have been investigated by various means, including the X-ray crystallography, Fourier transform infrared, electron paramagnetic resonance, and theoretical calculations.[10−26] It has been found that the Mn tetramer of OEC involves a double-oxo-bridged dinuclear manganese structure (Mn-(μ-O)$_2$-Mn).[8]

To mimic the active site of OEC, a number of high-valent multinuclear manganese complexes which have the oxo-bridged structure and are capable of catalyzing water oxidation have been proposed.[27−38] For instance, Limburg et al. have reported a prototypical dimanganese complex, $[H_2O(terpy)Mn^{III}(\mu\text{-}O)_2Mn^{IV}(terpy)OH_2](NO_3)_3$ (terpy = 2,2′:6′,2″-terpyridine), which is termed as complex **1** hereafter.[27] The geometric structure of complex **1** is sketched in Figure 1. It has been demonstrated that complex **1** is capable of splitting water and releasing oxygen in the presence of primary oxidants such as Ce^{4+},[32,39,40] $NaClO_4$,[27,28] or $KHSO_5$[28,41] or alternatively by electrochemical means.[42,43]

Since its synthesis, complex **1** has attracted much interest, because of its particular importance to the understanding of catalysis mechanism for oxygen evolution. As key components of complex **1**, the two manganese centers play essential roles in the water oxidation process, and their relevant chemical

Received: November 23, 2012
Published: January 17, 2013

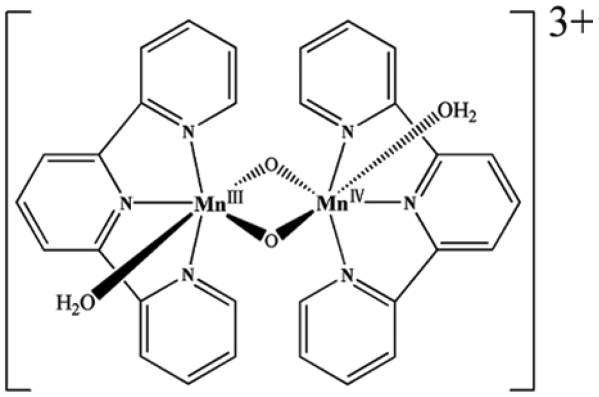

Figure 1. A sketch for the structure of $[H_2O(terpy)Mn^{III}(\mu\text{-}O)_2Mn^{IV}(terpy)OH_2]^{3+}$ (terpy = 2,2′:6′,2″-terpyridine), which is referred to as complex **1** in this paper.

properties, such as the oxidation and spin states, have been studied by experiments[27,28,42,44−46] and calculations.[47−51] For instance, Wang and co-workers have characterized the oxidation of inorganic core $[Mn^{III}(\mu\text{-}O)_2Mn^{IV}]^{3+}$ by carrying out density-functional theory (DFT) calculations for the free energy changes associated with the involving chemical processes.[47] Their computational results were consistent with cyclic voltammogram (CV) measurements,[43] indicating that the oxidation of complex **1** in water occurs through a proton coupled electron transfer (PCET) process.

Aside from the difference in charge and spin states of the two manganese centers, their surrounding chemical environment is considered to be quite similar. This is because of the overall symmetric coordination topology around the dimanganese ions, as well as the homogeneity of water solvent. Nevertheless, the subtle structural and chemical asymmetry may lead to significant distinction for the two manganese centers, in terms of their roles in the water splitting and oxygen evolution processes. This has been manifested in a variety of intriguing issues in the literature.

For instance, Cady and co-workers[43] have examined the electrochemical behavior of complex **1** in water under a variety of pH and buffered conditions. They have found that in the presence of acetate buffer, one (and only one) of the terminal water ligands bound to manganese is replaced by an acetate anion, and such single acetate binding occurs at the Mn(IV) center. Wang and co-workers[47] have carried out DFT calculations to obtain the thermodynamic energetics related to the acetate binding. By comparing the free energy change for replacing the terminal water ligand bound to Mn(IV) and that to Mn(III), they concluded that the preferential acetate binding site is Mn(IV), which agrees with Cady et al.'s conclusion. However, recently Milikisiyants and co-workers[45] have probed the intramolecular magnetic interactions of complex **1** using two-dimensional hyperfine sublevel correlation (HYSCORE) spectroscopy. They have demonstrated that the two protons of the water ligand coordinated at Mn(III) are magnetically equivalent, whereas the Mn(IV) counterparts are inequivalent. Based on this, they have measured the HYSCORE spectra of **1** in acetate buffer and concluded that the acetate replaces the terminal water coordinated at Mn(III). This is clearly contrary to the conclusion of Cady et al.[43] and Wang et al.[47] This apparent inconsistency among existing literature reports highlights the nontrivial structural and chemical asymmetry of the two manganese ions.

Being close to the manganese centers, the μ-oxo bridges of complex **1** may exhibit a certain level of asymmetry in both geometric structure and chemical functionality. In aqueous solution, they are likely to be involved in the catalysis of oxygen evolution.[48] Lundberg and co-workers have proposed that the coordination of a water molecule to an oxo-bridge is a key step for the O−O bond formation.[49,50] In a recently proposed reaction model by Hatakeyama and co-workers,[51] the formation of a hydrogen bond between an oxo-bridge and a primary oxidant molecule is crucial to the oxygen evolution.[51] Since the two bridge oxygen atoms of complex **1** are not entirely equivalent, it is important to explore their chemical similarity and asymmetry, so as to understand the underlying mechanism of their interactions with the aqueous environment.

To provide valuable insight into the issues raised above, in this work we investigate the intrinsic asymmetry of the dimanganese ion core $[Mn^{III}(\mu\text{-}O)_2Mn^{IV}]^{3+}$ by carrying out first-principles calculations at the DFT level. Based on the calculation results, the difference versus similarity in geometric and electronic structures around the two manganese centers are analyzed in detail. Discussions will focus on elucidating the influences of asymmetry features on the chemical functions of each individual manganese center in complex **1**. In particular, the apparent inconsistency in the preferential acetate binding site is resolved.

The remainder of this paper is organized as follows. Section II outlines the computational methods for calculating the geometric and electronic structures of complex **1** and relevant species. Section III presents the detailed calculation results, which are then connected to experimental findings in the literature. Section IV gives the concluding remarks.

II. COMPUTATIONAL METHODS

All the DFT calculations are carried out using the Gaussian09 program.[52] The hybrid B3LYP exchange-correlation functional[53,54] is used to determine the geometric and electronic structures. The geometry optimization and subsequent frequency analysis are performed with a mixed basis set: the LanL2DZ basis[55] with effective core potential for the Mn atoms, the 6-31G(2df) basis including two polarization functions for μ-oxo oxygen atoms, and the 6-31G basis for the rests. Further increasing the size of the basis set has only a minor effect on the optimized structures. The energetic data of dimanganese species are extracted from the single-point calculations done at the optimized geometries, with a much more extensive basis set: the LanL2DZ basis for the Mn atoms and the correlation consistent cc-pVTZ basis[56,57] for all the other atoms.

It is well-known that the minimum energy configuration of complex **1** in a DFT treatment involves a broken symmetry (BS) state,[47,49] where the unpaired *d*-electrons localized on the two manganese ions are in spin-α and β states, respectively. Our calculations affirm that the BS spin arrangement indeed yields the energetically most stable ground state, and hence the BS state is adopted for the involving dimanganese complexes throughout this work. The Mulliken population analysis is employed to estimate the partial charge and spin distribution on each atom.

To account for the solvation effects due to water environment, the solvation free energy is calculated by using the polarizable continuum model (PCM) of Tomasi and co-workers[58] and with the same mixed basis set as that adopted for geometry optimization. In addition to the implicit water solvent

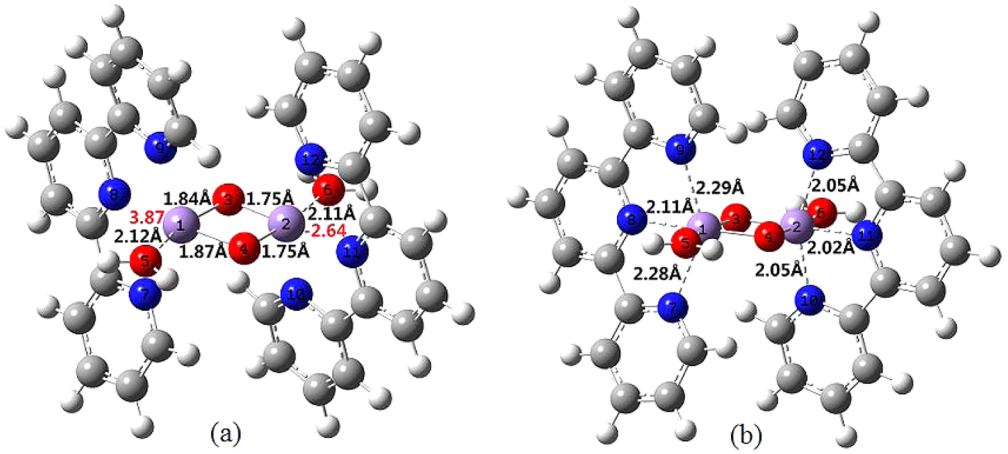

Figure 2. Optimized structure of complex **1** in BS ground state, with Mn(III) and Mn(IV) labeled as Mn1 and Mn2, respectively. The purple, red, blue, gray, and white balls represent Mn, O, N, C, and H atoms, respectively. Panels (a) and (b) display complex **1** in different orientations. The Mulliken spin populations on Mn1 and Mn2 (numbers in red) and the distances between the Mn centers and oxo-bridge oxygen atoms are shown in (a). The distances between the Mn centers and neighboring nitrogen atoms on terpyridyl ligand are displayed in (b).

treated by PCM, "explicit" water molecules are included in the studies of hydrogen bonding with the oxo-bridge oxygen atoms.

The above computational method is verified by calculating the thermodynamic energetics associated with the oxidation of **1**, i.e., $Mn^{III}Mn^{IV} \rightarrow Mn^{IV}Mn^{IV}$ ($\mathbf{1}_{ox}$), in aqueous solution. The resulting redox potential for the $\mathbf{1} \rightarrow \mathbf{1}_{ox}$ conversion and its pH-dependence agree reasonably with previous experimental and theoretical studies.[43,47] In particular, the pK_a of the terminal water ligand bound to manganese centers of $\mathbf{1}_{ox}$ has been determined to be 1.8 by CV measurement,[43] while in our calculations, it is obtained as 1.2 from the free energy change associated with the deprotonation of water ligand through a Born−Haber cycle.[59] This thus affirms that the DFT-B3LYP method is sufficiently accurate for predicting the thermodynamic properties of complex **1** and related species.

III. RESULTS AND DISCUSSIONS

1. Asymmetry Features in Geometric and Electronic Structures of Manganese Centers. Figure 2 depicts the optimized structure of complex **1**, where the distances between each manganese center and its surrounding oxygen and nitrogen atoms are highlighted. By employing the Mulliken analysis, the partial charges are determined to be 1.19 and 1.28, and the corresponding spin populations are 3.87 and −2.64 on Mn(III) and Mn(IV) centers, respectively. This affirms that the electronic ground state of **1** is indeed a BS state, which involves four unpaired spin-α *d*-electrons localized on Mn(III) and three spin-β *d*-electrons on Mn(IV), respectively. The asymmetry in electronic structure is clearly manifested through the difference in charge and spin densities at the two manganese centers. Although the local charges on high-valent Mn ions are largely compensated by intramolecular coordination bonding and electron polarization, the positive charges are not completely neutralized. In particular, the Mn(IV) ion carries slightly more positive charges than the Mn(III). Consequently, an external anion is expected to be energetically more favorable to be bound to Mn(IV), due to the stronger electrostatic interaction.

The structural asymmetry associated with the two manganese centers of **1** is clearly indicated in Figure 2, where the Mn(III)−O bond length is more than 0.1 Å longer than that of Mn(IV)−O, and the average distance between the Mn(III) ion and its surrounding nitrogen atoms at the nearby terpyridyl ligand is almost 0.2 Å larger than the Mn(IV) counterpart. Therefore, the Mn(III) core is overall farther away from the surrounding atoms, leaving a relatively larger "pocket" formed by oxo-bridges and neighboring terpyridyl and coordinated water ligands, as compared to the Mn(IV) center. Note that such structural asymmetry is largely suppressed in the crystal of complex **1**.[27] This may be because of the compact packing of **1** under strong intermolecular interactions.

The asymmetry in geometric structure would lead to a conspicuous difference in chemical reactivity of the two manganese centers. For instance, the size of "pocket" determines crucially the steric effects for reactions occurring at the metal center inside. In the case of complex **1**, the larger size of the "pocket" around Mn(III) ion implies that it is easier for an external molecule to enter its surrounded area and interact with it.

Interestingly, in the case of single acetate binding to complex **1**, the asymmetry features in electronic and geometric would have exactly opposite effects on the preferential binding site. While the electrostatic interaction favors binding to Mn(IV), the steric effect advocates the coordination occurs at Mn(III). Both these two aspects are to be investigated in detail and addressed later in Section III 3.

2. Influence of Water Environment and Hydrogen Bonding around Manganese Centers. In addition to the asymmetry features of complex **1** itself, the presence of water solvent may also influence the chemical properties of the two manganese centers. This includes the electrostatic interactions and the formation of hydrogen bonds between **1** and surrounding water molecules. The dielectric response of **1** to water solvent is treated by using the implicit solvent model (PCM). The dimanganese ion core is stabilized through electron density redistribution.

We then proceed to explore the second effect of water solvent, the formation of hydrogen bond near around the manganese centers. Both oxo-bridge oxygen atoms on complex **1** carry negative partial charges. The Mulliken charges are calculated to be −0.75 and −0.73 for O3 and O4, respectively. Therefore, hydrogen bonding with external water molecules will lower the total energy and further stabilize complex **1**. In the following we consider two scenarios of hydrogen bond formation: (i) a single water molecule is hydrogen-bonded to a

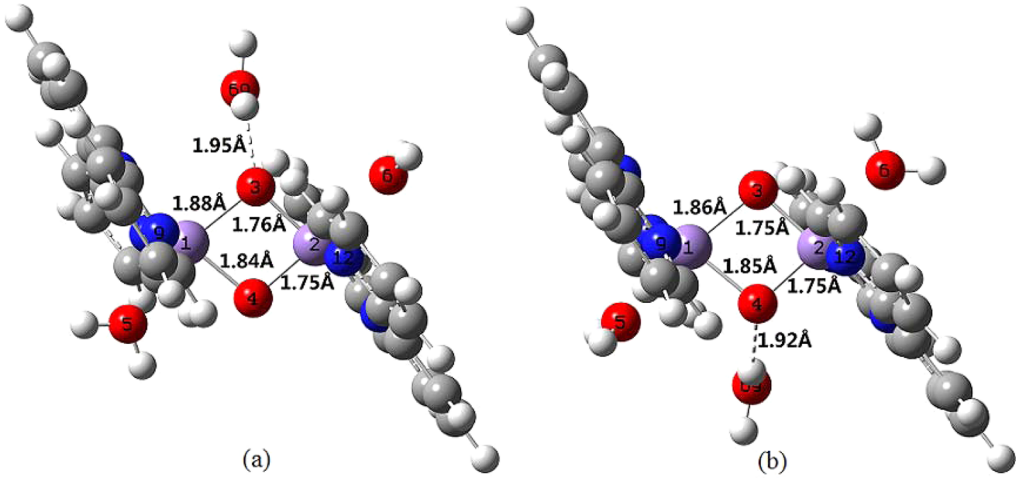

Figure 3. Optimized structure of complex **1** with an external water molecule attached to a μ-oxo oxygen atom through hydrogen bonding. Panels (a) and (b) display the two cases where the external water molecule is attached to O3 and O4, respectively.

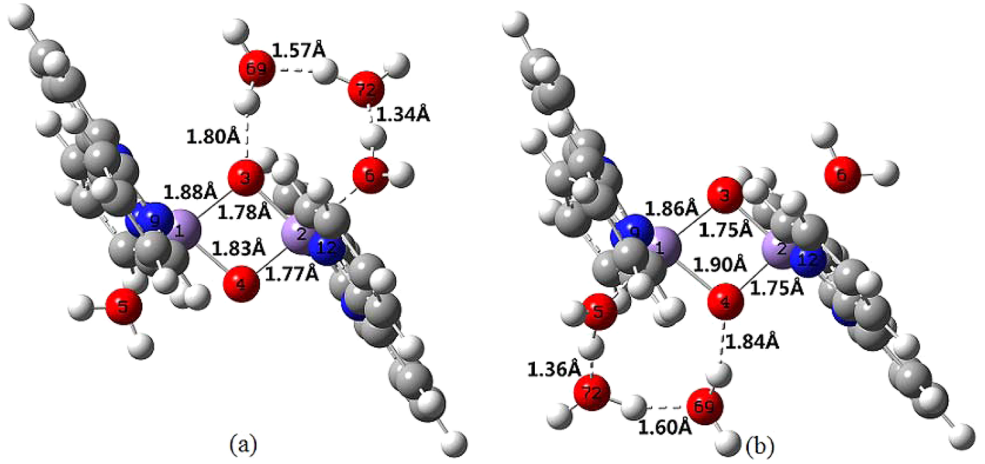

Figure 4. Optimized structure of complex **1** with two external water molecules linking an oxo-bridge oxygen atom to a terminal water ligand through hydrogen bonding. Panels (a) and (b) display the two cases where an external water molecule is attached to O3 and O4, respectively.

μ-oxo oxygen atom, which has been observed in experiments,[27,44] and (ii) a closed loop linking a μ-oxo oxygen atom to a terminal water ligand is formed, which consists of three hydrogen bonds mediated by two external water molecules.

For scenario (i), the optimized structures of **1** with an external water molecule bound to O3 and O4 are displayed in Figure 3 (parts (a) and (b), respectively). In both cases, the external water resides right on top of the μ-oxo oxygen atom that it is bound to, and the water molecular plane is almost perpendicular to the plane of the di-μ-oxo core. The external water molecule bound to O3 (O4) occupies the "pocket" space around Mn(IV) [Mn(III)] and forces the corresponding terminal water ligand to rotate so as to minimize the steric repulsion. The free energy change associated with the hydrogen bonding at O4 is calculated to be 1.6 kcal/mol lower than that at O3. This may be because of the larger "pocket" size around Mn(III) center. Such an energy difference is actually rather small under room temperature. Noting also the fact that the geometry of hydrogen bonding (such as both length and orientation) in both cases is almost identical, we conclude that the water solvent has symmetric influence on the two manganese centers.

For scenario (ii), Figure 4(a),(b) depicts the optimized geometries with the hydrogen-bond loop formed at O3 and O4, respectively. It has been found in previous experiments that, for the crystalline phase of **1**, the μ-oxo bridges and coordinated water ligands are interlocked by hydrogen-bonding water molecules.[27] The stabilized structures displayed in Figure 4 affirm that such hydrogen bonding patterns may also exist in the solution phase. Analogous to scenario (i), the two external water molecules mediating the hydrogen bonds fill the "pocket" around the Mn(IV) or Mn(III) center, and the hydrogen-bond loops exhibit nearly identical fine structures in both cases. Based on our calculations, the two molecular clusters sketched in Figure 4(a),(b) are almost degenerate in free energy, with a rather minor difference of 0.96 kcal/mol. Therefore, we conclude that the influence of water solvent on the two distinct manganese centers is overall symmetric, even with multiple water molecules included explicitly into the computation model.

Based on the above analysis, we affirm that the homogeneous water environment has a rather minor contribution to the structural/chemical asymmetry of the two metal ions. Consequently, the difference in chemical function between the two manganese centers originates mostly from the intrinsic asymmetry features of complex **1**, as discussed in Section III 1.

3. Preferential Binding Site for Acetate in Replacement of a Terminal Water Ligand. Now we are in the

$$[(H_2O)(terpy)Mn^{III}(\mu\text{-}O)_2Mn^{IV}(terpy)(OH_2)]^{3+} + AcO^- \xrightarrow{\Delta G_1=-0.92\ eV} [AcO(terpy)Mn^{III}(\mu\text{-}O)_2Mn^{IV}(terpy)(OH_2)]^{2+} + H_2O \quad (a)$$

$$[(H_2O)(terpy)Mn^{III}(\mu\text{-}O)_2Mn^{IV}(terpy)(OH_2)]^{3+} + AcO^- \xrightarrow{\Delta G_2=-0.97\ eV} [(H_2O)(terpy)Mn^{III}(\mu\text{-}O)_2Mn^{IV}(terpy)AcO]^{2+} + H_2O \quad (b)$$

Figure 5. Free energy changes for an acetate (AcO^-) binding to complex **1**. (a) and (b) correspond to the cases where AcO^- replaces the terminal water ligand coordinated at Mn(III) and Mn(IV) centers, respectively.

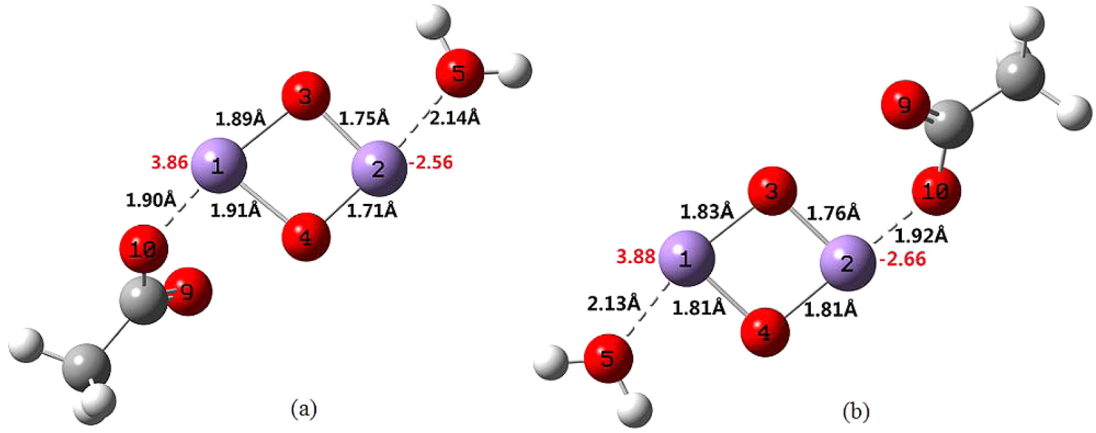

Figure 6. Structural details of μ-oxo-bridged dimanganese complexes with an AcO^- replacing the water ligand at (a) Mn(III) and (b) Mn(IV) center. For clarity, all terpyridyl ligands are omitted in the visualization. The Mulliken spin populations on the two manganese centers are labeled in red. In the both complexes, Mn1 and Mn2 represent Mn(III) and Mn(IV) centers, respectively. The Mulliken analysis verifies our designation of apparent valence charges for the Mn atoms.

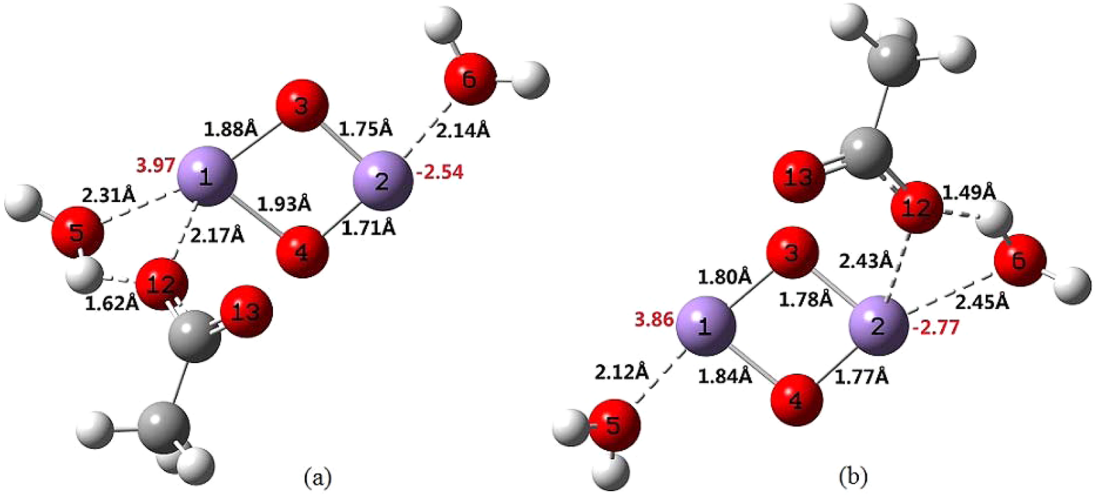

Figure 7. Structural details of (a) TS1 and (b) TS2 complexes, where the acetate anion is bound to Mn(III) and Mn(IV) center, respectively. For clarity, all terpyridyl ligands are omitted in the visualization. The Mulliken spin populations on the two manganese centers are labeled in red.

position to resolve the controversy on the preferential binding site at complex **1** for an acetate anion (AcO^-). Since the influence of aqueous environment is overall symmetric on the both manganese centers, we only need to focus on two aspects: the asymmetry in (i) local electrophilicity and in (ii) local steric effects.

Figure 5 illustrates the single acetate binding to Mn(IV) or Mn(III) center. The associated free energy changes are calculated to be −0.97 and −0.92 eV, respectively. Consequently, the acetate binding to Mn(IV) is only 1.0 kcal/mol more stable than to Mn(III). In the previous study of Wang et al.,[47] the free energy changes for acetate binding reactions presented in Figure 5(a),(b) were calculated to be −0.22 eV and −1.01 eV, respectively. While the latter agrees reasonably with our result, the former is conspicuously higher. This might be because the structure of the $[AcO{-}Mn(III)]^{2+}$ complex had not been fully relaxed.

The optimized geometries of AcO^- coordinated dimanganese complexes are depicted in Figure 6, where all the terpyridyl ligands are omitted in the visualization to highlight the coordination of AcO^-. The two complexes displayed in Figure 6(a),(b) are well distinguishable, as indicated by their distinct structural details, as well as the characteristic spin densities at the two Mn centers. Meanwhile, their energy difference is negligibly small under room temperature. This is thus consistent with the fact that the local electrophilicity (manifested by Mulliken charge populations) of the two Mn ions deviate only slightly from each other. Therefore, from the thermodynamic perspective, the acetate bound to Mn(IV) or to Mn(III) is almost equally probable.

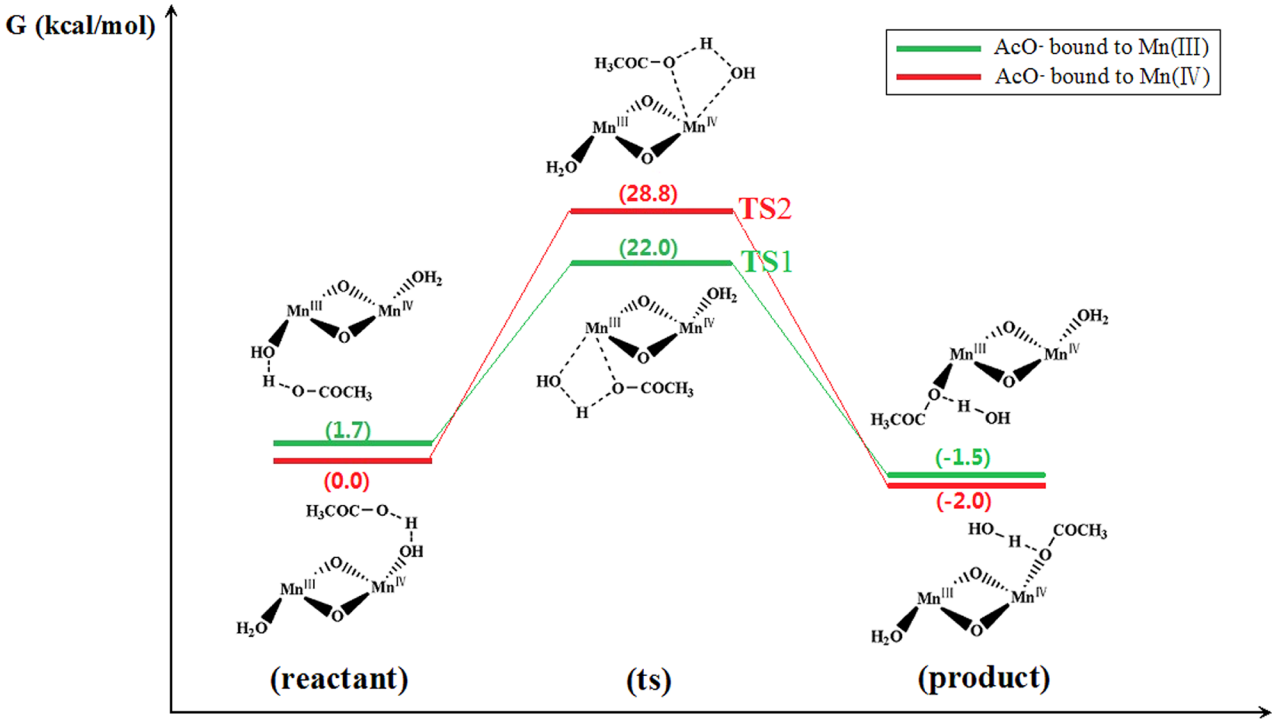

Figure 8. Schematic diagram of two possible pathways for the acetate binding reaction. The relative free energies of all the involving species are shown, where the free energy of reactant state complex with AcO^- near to Mn(IV) is set to zero.

We then evaluate how the asymmetry in local steric effects influences the acetate binding process. It should be emphasized that the AcO^- is a relatively small molecule, as compared to the size of "pocket" vacancy around a manganese center. As a result, an AcO^- is likely to enter the "pocket" and approach to the manganese ion, while the coordinated water ligand leaves simultaneously. In other words, the acetate binding reaction involves a cooperative mechanism between the AcO^- and water ligand. Such a reaction mechanism requires a much lower activation than that associated with a sequential process where the dissociation of terminal water precedes the approaching of AcO^-. Moreover, a hydrogen bond is formed between the AcO^- and water ligand in the transition state (TS) of the overall complex and thus further reduces the activation free energy.

The QST3 algorithm of Gaussian09 program is used to search for the TS geometries. The obtained TS complexes are verified by frequency analysis as indeed the saddle points of energy surface, as there is one and only one imaginary frequency corresponding to the attachment of AcO^-. Figure 7(a),(b) displays the structural details of the TS complexes (referred to as TS1 and TS2 hereafter), with the AcO^- approaching the Mn(III) and Mn(IV) center, respectively. In both TS1 and TS2, the distance from the Mn center to AcO^- is similar to that to water ligand. A hydrogen bond is formed between the water ligand and an oxygen atom of AcO^-. Meanwhile, the other oxygen atom of AcO^- also interacts with a hydrogen atom at its neighboring terpyridine through a weaker hydrogen bond (not shown).

Aside from the above common structural features, it is more important to address the differences between the two TS complexes. It should be accentuated that the distance between AcO^- and Mn ion in TS1 is significantly shorter (by as much as 0.25 Å) than the TS2 counterpart, and so is the distance between the leaving water ligand and Mn ion. This is due to the relatively smaller "pocket" size associated with the Mn(IV) center of complex **1**, which prevents the AcO^- and water ligand from getting closer to the Mn(IV) ion. Moreover, the stronger steric repulsion associated with the Mn(IV) center makes the free energy of TS2 significantly higher than that of TS1 (by as much as 6.8 kcal/mol). This would result in a much slower rate for acetate binding reaction via TS2 than via TS1. Therefore, from the kinetic perspective, the Mn(III) center is the predominant binding site for the AcO^-.

The two possible pathways (via TS1 and TS2) for the acetate binding to complex **1** are plotted in parallel in the schematic diagram of Figure 8. The reactant states are composite complexes $[AcO...\mathbf{1}]^{2+}$, where (...) represents a hydrogen bond linking the AcO^- to a terminal water ligand of **1**. In the product states, a terminal water ligand is replaced by the AcO^-, with their hydrogen bond in between preserved. The free energy of the reactant-state complex with AcO^- near the Mn(IV) center is set to zero, and the relative free energies of all involving species are evaluated and displayed in Figure 8.

The two reactant (product) states differ by only 0.7 (0.5) kcal/mol in free energy. This affirms that the two possible pathways are thermodynamically almost equivalent. On the other hand, the free energy of TS2 is much higher than that of TS1. The activation energies associated with the pathways via TS1 and TS2 are evaluated to be 20.3 and 28.8 kcal/mol, respectively. This amounts to a drastic difference in reaction rate (around 7 orders of magnitude) between the two pathways. In particular, the activation energy for TS2 is too high to overcome under the room temperature. Therefore, the acetate binding should occur predominantly via TS1, and the resulting product should be a complex with AcO^- coordinated at the Mn(III) center. This thus agrees with the recent experimental finding of Milikisiyants et al.[44] and finally resolves the controversy about the preferential acetate binding site at complex **1**.

To examine the dispersive effects on the binding of AcO^- to complex **1**, we recalculate the electronic energies of all the related species in Figure 8 with the B97D method,[60] which includes an empirical dispersion energy correction. The resulting energy diagram for the two possible reaction pathways is qualitatively similar to Figure 8 (see the Supporting Information for details). The energy differences between the reactant, TS, and product states of the two possible pathways are 0.9, 5.2, and 0.5 kcal/mol with the B97D method, which agree consistently with the B3LYP prediction of 1.7, 6.8, and 0.5 kcal/mol. This clearly affirms that the dispersive interactions have only minor effects on the mechanism of acetate binding to complex **1**.

IV. CONCLUDING REMARKS

In this work, we have carried out DFT calculations on a biomimetic dimanganese complex as a structural model for the OEC of PSII. The B3LYP exchange-correlation functional is used, with the solvent environment treated by the PCM. The calculation results provide useful insights into the structural and chemical asymmetry for the two manganese centers of complex **1**, based on which we resolve the controversy in the literature on the preferential acetate binding site at **1**.

Our calculations have indicated that the water environment has almost symmetric influence on the Mn(III) and Mn(IV) centers of complex **1**, even with the formation of hydrogen bonds considered explicitly. Consequently, the chemical functions of **1** are largely determined by the intrinsic features of its geometric and electronic structures. In particular, the Mn(IV) center of **1** is found to be slightly more electrophilic than the Mn(III) center, and meanwhile, it imposes significantly larger steric repulsion for a molecule or ligand. For the issue of preferential acetate binding site, we conclude that the steric effect plays a decisive role, which leads to the predominant coordination of AcO^- at the Mn(III) center.

The analysis on structural and chemical asymmetry of a multicenter complex can be extended to elucidate the mechanisms of various chemical processes involving metal−ligand interactions. In particular, for reactions with multiple possible channels, both the thermodynamic and kinetic aspects need to be considered, and their impacts on the pathways are to be evaluated comprehensively. In these cases, the studies on asymmetry features will shed important light on the key factors that bias the reactions. Specifically, for the biomimetic water-splitting complex **1**, it would be interesting to know how the structural and chemical asymmetry will affect its functionality upon adsorption onto semiconductor or electrode surfaces, as in realistic photosynthetic applications. Progress along this direction is underway.

■ ASSOCIATED CONTENT

Supporting Information

The details about the computational methods, the geometric structures of complex **1** and related species, the Mulliken charge and spin population analysis, and the frequency analysis for transition state complexes. This material is available free of charge via the Internet at http://pubs.acs.org.

■ AUTHOR INFORMATION

Corresponding Author

*E-mail: xz58@ustc.edu.cn.

Notes

The authors declare no competing financial interest.

■ ACKNOWLEDGMENTS

The support from the Natural Science Foundation of China (Grant No. 21103157 and No. 21233007) and the Fundamental Research Funds for Central Universities (Grant No. 2340000025 and No. 2340000034) is gratefully acknowledged.

■ REFERENCES

(1) Meyer, T. J. *Acc. Chem. Res.* **1989**, *22*, 163−170.
(2) Manchanda, R.; Brudvig, G. W.; Crabtree, R. H. *Coord. Chem. Rev.* **1995**, *144*, 1−38.
(3) Kok, B.; Forbush, B.; McGloin, M. P. *Photochem. Photobiol.* **1970**, *11*, 457−475.
(4) McEvoy, J. P.; Brudvig, G. W. *Chem. Rev.* **2006**, *106*, 4455−4483.
(5) Kulik, L. V.; Epel, B.; Lubitz, W.; Messinger, J. *J. Am. Chem. Soc.* **2007**, *129*, 13421−13435.
(6) Ferreira, K. N.; Iverson, T. M.; Maghlaoui, K.; Barber, J.; Iwata, S. *Science* **2004**, *303*, 1831−1838.
(7) Mishra, A.; Wernsdorfer, W.; Abboud, K. A.; Christou, G. *Chem. Commun.* **2005**, *1*, 54−56.
(8) Yachandra, V. K.; Sauer, K.; Klein, M. P. *Chem. Rev.* **1996**, *96*, 2927−2950.
(9) Yano, J.; Kern, J.; Sauer, K.; Latimer, M. J.; Pushkar, Y.; Biesiadka, J.; Loll, B.; Saenger, W.; Messinger, J.; Zouni, A.; Yachandra, V. K. *Science* **2006**, *314*, 821−825.
(10) Mukhopadhyay, S.; Mandal, S. K.; Bhaduri, S.; Armstrong, W. H. *Chem. Rev.* **2004**, *104*, 3981−4026.
(11) Umena, Y.; Kawakami, K.; Kamiya, N.; Shen, J.-R. *Nature* **2011**, *473*, 55−60.
(12) Kawakami, K.; Umena, Y.; Kamiya, N.; Shen, J.-R. *J. Photochem. Photobiol., B* **2011**, *104*, 9−18.
(13) Zouni, A.; Witt, H.-T.; Kern, J.; Fromme, P.; Kraub, N.; Saenger, W.; Orth, P. *Nature* **2001**, *409*, 739−743.
(14) Noguchi, T.; Ono, T.; Inoue, Y. *Biochim. Biophys. Acta* **1995**, *1228*, 189−200.
(15) Chu, H.-A.; Sackett, H.; Babcock, G. T. *Biochemistry* **2000**, *39*, 14371−14376.
(16) Carrell, T. G.; Tyryshkin, A. M.; Dismukes, G. C. *J. Biol. Inorg. Chem.* **2002**, *7*, 2−22.
(17) Cady, C. W.; Crabtree, R. H.; Brudvig, G. W. *Coord. Chem. Rev.* **2008**, *252*, 444−455.
(18) Wu, A. J.; Penner-Hahn, J. E.; Pecoraro, V. L. *Chem. Rev.* **2004**, *104*, 903−938.
(19) Mukhopadhyay, S.; Mandal, S. K.; Bhaduri, S.; Armstrong, W. H. *Chem. Rev.* **2004**, *104*, 3981−4026.
(20) Rapatskiy, L.; Cox, N.; Savitsky, A.; Ames, W. M.; Sander, J.; Nowaczyk, M. M.; Rögner, M.; Boussac, A.; Neese, F.; Messinger, J.; Lubitz, W. *J. Am. Chem. Soc.* **2012**, *134*, 16619−16634.
(21) Cox, N.; Rapatskiy, L.; Su, J.-H.; Pantazis, D. A.; Sugiura, M.; Kulik, L.; Dorlet, P.; Rutherford, A. W.; Neese, F.; Boussac, A.; Lubitz, W.; Messinger, J. *J. Am. Chem. Soc.* **2011**, *133*, 3635−3648.
(22) Stich, T. A.; Yeagle, G. J.; Service, R. J.; Debus, R. J.; Britt, R. D. *Biochemistry* **2011**, *50*, 7390−7404.
(23) Kusunoki, M. *Biochim. Biophys. Acta* **2007**, *1767*, 484−492.
(24) Dau, H.; Zaharieva, I. *Acc. Chem. Res.* **2009**, *42*, 1861−1870.
(25) Dau, H.; Grundmeier, A.; Loja, P.; Haumann, M. *Philos. Trans. R. Soc. London, Ser. B* **2008**, *363*, 1237−1244.
(26) Siegbahn, P. E. M. *Acc. Chem. Res.* **2009**, *42*, 1871−1880.
(27) Limburg, J.; Vrettos, J. S.; Liable-Sands, L. M.; Rheingold, A. L.; Crabtree, R. H.; Brudvig, G. W. *Science* **1999**, *283*, 1524−1527.
(28) Limburg, J.; Vrettos, J. S.; Chen, H. Y.; de Paula, J. C.; Crabtree, R. H.; Brudvig, G. W. *J. Am. Chem. Soc.* **2001**, *123*, 423−430.
(29) Mullins, C. S.; Pecoraro, V. L. *Coord. Chem. Rev.* **2008**, *252*, 416−443.

(30) Yagi, M.; Syouji, A.; Yamada, S.; Komi, M.; Yamazaki, H.; Tajima, S. *Photochem. Photobiol. Sci.* **2009**, *8*, 139−147.
(31) Yamazaki, H.; Shouji, A.; Kajita, M.; Yagi, M. *Coord. Chem. Rev.* **2010**, *254*, 2483−2491.
(32) Yagi, M.; Narita, K. *J. Am. Chem. Soc.* **2004**, *126*, 8084−8085.
(33) Poulsen, A. K.; Rompel, A.; McKenzie, C. J. *Angew. Chem., Int. Ed.* **2005**, *44*, 6916−6920.
(34) Shimazaki, Y.; Nagano, T.; Takesue, H.; Ye, B.-H.; Tani, F.; Naruta, Y. *Angew. Chem., Int. Ed.* **2004**, *43*, 98−100.
(35) Ruettinger, W.; Yagi, M.; Wolf, K.; Bernasek, S.; Dismukes, G. C. *J. Am. Chem. Soc.* **2000**, *122*, 10353−10357.
(36) Brimblecombe, R.; Koo, A.; Dismukes, G. C.; Swiegers, G. F.; Spiccia, L. *J. Am. Chem. Soc.* **2010**, *132*, 2892−2894.
(37) Chen, H. M.; Chen, C. K.; Liu, R.-S.; Zhang, L.; Zhang, J.; Wilkinson, D. P. *Chem. Soc. Rev.* **2012**, *41*, 5654−5671.
(38) Kurz, P.; Berggren, G.; Anderlund, M. F.; Styring, S. *Dalton Trans.* **2007**, *38*, 4258−4261.
(39) Narita, K.; Kuwabara, T.; Sone, K.; Shimizu, K.; Yagi, M. *J. Phys. Chem. B* **2006**, *110*, 23107−23114.
(40) Tagore, R.; Chen, H. Y.; Zhang, H.; Crabtree, R. H.; Brudvig, G. W. *Inorg. Chim. Acta* **2007**, *360*, 2983−2989.
(41) Tagore, R.; Crabtree, R. H.; Brudvig, G. W. *Inorg. Chem.* **2008**, *47*, 1815−1823.
(42) Li, G. H.; Sproviero, E. M.; Snoeberger, R. C., III; Iguchi, N.; Blakemore, J. D.; Crabtree, R. H.; Brudvig, G. W.; Batista, V. S. *Energy Environ. Sci.* **2009**, *2*, 230−238.
(43) Cady, C. W.; Shinopoulos, K. E.; Crabtree, R. H.; Brudvig, G. W. *Dalton Trans.* **2010**, *39*, 3985−3989.
(44) Milikisiyants, S.; Chatterjee, R.; Lakshmi, K. V. *J. Phys. Chem. B* **2011**, *115*, 12220−12229.
(45) Chatterjee, R.; Milikisiyants, S.; Lakshmi, K. V. *Phys. Chem. Chem. Phys.* **2012**, *14*, 7090−7097.
(46) Mukhopadhyay, S.; Mandal, S. K.; Bhaduri, S.; Armstrong, W. H. *Chem. Rev.* **2004**, *104*, 3981−4026.
(47) Wang, T.; Brudvig, G. W.; Batista, V. S. *J. Chem. Theory Comput.* **2010**, *6*, 2395−2401.
(48) Wang, T.; Brudvig, G. W.; Batista, V. S. *J. Chem. Theory Comput.* **2010**, *6*, 755−760.
(49) Lundberg, M.; Blomberg, M. R. A.; Siegbahn, P. E. M. *Inorg. Chem.* **2004**, *43*, 264−274.
(50) Lundberg, M.; Siegbahn, P. E. M. *Chem. Phys. Lett.* **2005**, *401*, 347−351.
(51) Hatakeyama, M.; Nakata, H.; Wakabayashi, M.; Yokojima, S.; Nakamura, S. *J. Phys. Chem. A* **2012**, *116*, 7089−7097.
(52) Frisch, M. J.; Trucks, G. W.; Schlegel, H. B.; Scuseria, G. E.; Robb, M. A.; Cheeseman, J. R.; Scalmani, G.; Barone, V.; Mennucci, B.; Petersson, G. A.; Nakatsuji, H.; Caricato, M.; Li, X.; Hratchian, H. P.; Izmaylov, A. F.; Bloino, J.; Zheng, G.; Sonnenberg, J. L.; Hada, M.; Ehara, M.; Toyota, K.; Fukuda, R.; Hasegawa, J.; Ishida, M.; Nakajima, T.; Honda, Y.; Kitao, O.; Nakai, H.; Vreven, T.; Montgomery, J. A., Jr.; Peralta, J. E.; Ogliaro, F.; Bearpark, M.; Heyd, J. J.; Brothers, E.; Kudin, K. N.; Staroverov, V. N.; Kobayashi, R.; Normand, J.; Raghavachari, K.; Rendell, A.; Burant, J. C.; Iyengar, S. S.; Tomasi, J.; Cossi, M.; Rega, N.; Millam, J. M.; Klene, M.; Knox, J. E.; Cross, J. B.; Bakken, V.; Adamo, C.; Jaramillo, J.; Gomperts, R.; Stratmann, R. E.; Yazyev, O.;Austin, A. J.; Cammi, R.; Pomelli, C.; Ochterski, J. W.; Martin, R. L.; Morokuma, K.; Zakrzewski, V. G.; Voth, G. A.; Salvador, P.; Dannenberg, J. J.; Dapprich, S.; Daniels, A. D.; Farkas, O.; Foresman, J. B.; Ortiz, J. V.; Cioslowski, J.; Fox, D. J. *Gaussian 09, revision A.02*; Gaussian, Inc.: Wallingford, CT, 2009.
(53) Becke, A. D. *J. Chem. Phys.* **1993**, *98*, 5648−5652.
(54) Lee, C.; Yang, W.; Parr, R. G. *Phys. Rev. B* **1988**, *37*, 785−789.
(55) Hay, P. J.; Wadt, W. R. *J. Chem. Phys.* **1985**, *82*, 299−310.
(56) Dunning, T. H. *J. Chem. Phys.* **1989**, *90*, 1007−1023.
(57) Woon, D. E.; Dunning, T. H. *J. Chem. Phys.* **1993**, *98*, 1358−1371.
(58) Tomasi, J.; Mennucci, B.; Cammi, R. *Chem. Rev.* **2005**, *105*, 2999−3093.
(59) Bahers, T. L.; Adamo, C.; Ciofini, I. *Chem. Phys. Lett.* **2009**, *472*, 30−34.
(60) Grimme, S. *J. Comput. Chem.* **2006**, *27*, 1787−1799.